1 **Thresholds of fire response to moisture and fuel load differ between tropical savannas**

2 **and grasslands across continents**

3

4 Swanni T. Alvarado, Niels Andela, Thiago S. F. Silva, Sally Archibald

5

6 **Short running title:** Tropical savanna climate-fire responses

7

8 **Abstract**

9 **Aim:** An emerging framework for tropical ecosystems states that fire activity is either '*fuel*

10 *build-up limited*' or '*fuel moisture limited*' i.e. as you move up along rainfall gradients, the

11 major control on fire occurrence switches from being the amount of fuel, to the moisture

12 content of the fuel. Here we used remotely sensed datasets to assess whether interannual

13 variability of burned area is better explained by annual rainfall totals driving fuel build-up, or

14 by dry season rainfall driving fuel moisture.

15 **Location:** Pantropical savannas and grasslands

16 **Time period:** 2002-2016

17 **Methods:** We explored the response of annual burned area to interannual variability in

18 rainfall. We compared several linear models to understand how *fuel moisture* and *fuel build-*

19 *up effect* (accumulated rainfall during 6 and 24 months prior to the end of the burning season

20 respectively) determine the interannual variability of burned area and explore if tree cover,

21 dry season duration and human activity modified these relationships.

22 **Results:** Fuel and moisture controls on fire occurrence in tropical savannas varied across

23 continents. Only 24% of South American savannas were *fuel build-up limited* against 61% of

24 Australian savannas and 47% of African savannas. On average, South America switched from

25 fuel limited to moisture limited at 500 mm yr^{-1}, Africa at 800 mm yr^{-1} and Australia at 1000

26 mm yr^{-1} of mean annual rainfall.

27 **Main conclusions:** In 42% of tropical savannas (accounting for 41% of current area burned)

28 increased drought and higher temperatures will not increase fire, but there are savannas,

29 particularly in South America, that are likely to become more flammable with increasing

30 temperatures. These findings highlight that we cannot transfer knowledge of fire responses to

31 global change across ecosystems/regions – local solutions to local fire management issues are

32 required, and different tropical savanna regions may show contrasting responses to the same

33 drivers of global change.

1. Introduction

Understanding global controls on fire activity has become increasingly important in the context of ecosystem drying and climatic change (Jolly et al., 2015). In some ecosystems drought events and rising temperatures may exacerbate fire risk (Bowman et al., 2011; Price et al., 2015), and increase the incidence of large wildfires and fire-associated CO_2 emissions (Voulgarakis & Field, 2015; Hantson *et al.*, 2017). However, not all ecosystems burn more when exposed to drought and high temperatures. Pausas and Ribeiro (2013) showed that fire in lower-productivity systems was unresponsive to temperature, and paleo-records highlight regional differences in fire responses to changes in rainfall and temperature (Daniau *et al.*, 2012). Bradstock (2010) indicated that fire would respond to the factor that was most limiting in a particular ecosystem – and when there is no fuel to burn increased temperatures and drought conditions would be expected to have little impact on fire. Fires are therefore the outcome of complex interactions between climate, fire, vegetation and land management (Moritz *et al.*, 2012; Andela *et al.*, 2017; Forkel *et al.*, 2017; Abatzoglou *et al.*, 2018). Fire enabled Dynamic Global Vegetation Models (DGVMs) are designed to model these interactions, but model outcomes vary widely across models (Bowman *et al.*, 2014; Williams & Abatzoglou, 2016; van Marle *et al.*, 2017), based on a wide range of different parameterizations (Hantson *et al.*, 2016; Rabin *et al.*, 2017). The role of fire for carbon cycling and maintaining biodiversity under scenarios of future change therefore remain uncertain for tropical biomes.

Fire is an essential ecosystem process in tropical savannas and grasslands, which are characterized by high fire frequency under natural conditions (Bond *et al.*, 2005; Chuvieco *et al.*, 2008). Rainfall is the dominant control on fire activity in the tropics (van der Werf *et al.*, 2008); seasonal variation in tropical savanna rainfall typically results in vegetation production and biomass build-up during the wet season, followed by a dry period when dead or dormant herbaceous vegetation becomes flammable (Bradstock, 2010). The dynamic balance of productivity and seasonal drought also determines the interannual variability of burned area (Pausas & Ribeiro, 2013). In the humid tropics fire activity is constrained by fuel moisture conditions (*fuel moisture limited*) (Bradstock, 2010; Whitlock *et al.*, 2010): here negative rainfall anomalies increase fire activity by causing usually green, non-flammable vegetation to dry out sufficiently to carry fire (Aragão *et al.*, 2008). In contrast, in tropical biomes with low net primary productivity such as grasslands and xeric savannas, fire activity is constrained by fuel produced during the preceding growing seasons (*fuel build-up limited*)

(Whitlock *et al.*, 2010; O'Donnell *et al.*, 2011; Kahiu & Hanan, 2018): here anomalous wet years increase vegetation productivity which increases fire activity during the following dry seasons (Van Wilgen *et al.*, 2004; Archibald *et al.*, 2010; Pausas & Paula, 2012; Abatzoglou *et al.*, 2018).

Despite the important differences in fire ecology and behavior across fuel and moisture limited fire regimes, their global distribution remains unknown. While climate determines where and when fires can occur (van der Werf *et al.*, 2008; Archibald *et al.*, 2010), human land management modifies regional patterns of fire activity (Bistinas *et al.*, 2013; Andela *et al.*, 2017). Humans are a source of ignitions as fire is often used as a tool in pastoral and agricultural activities (Mistry, 2000; Cochrane & Ryan, 2009), but humans also alter fire sizes by increasing landscape fragmentation and changing the timing of ignitions (Le Page *et al.*, 2010). Moreover, there is evidence that the sensitivity of fire regimes to climate variability depends on human activities (Archibald *et al.*, 2010), as humans can "buffer" ecosystems (Bird *et al.*, 2012) from climate and fire extremes through the way that they manage landscapes and light fires (Yibarbuk *et al.*, 2002; Price *et al.*, 2012; Bird *et al.*, 2016). Vegetation cover and type also interact with fire, as grasses produce fine fuels that carry savanna fires. Tree cover in turn, may reduce fire occurrence by limiting grass productivity (Bond *et al.*, 2005; Hoffmann *et al.*, 2012; Aleman & Staver, 2018). The effects of climate and human land management on fire activity are therefore further modified by vegetation type, its cover and productivity (Archibald *et al.*, 2009; Bistinas *et al.*, 2014; Lehmann *et al.*, 2014).

Here we use satellite observations to study burned area-rainfall relationships across a moisture gradient, ranging from xeric grasslands to mesic tropical savannas. First, we identify pantropical rainfall thresholds where savanna and grassland fire regimes switch from *fuel build-up limited* to *fuel moisture limited*. Second, we investigate how these thresholds vary across regions and how spatial patterns in *fuel build-up-* and *fuel moisture limited* fire regimes are modified by rainfall seasonality, human activity, and tree cover. Understanding how climate, human activity, and ecosystem structure modify the response of fire activity to changing weather conditions is critical to model and forecast future fire activity across different environments.

2. Data and methods

2.1. Remote sensing data

101   For our analysis, we rescaled all data to 0.25° spatial resolution by calculating the mean value,

102   land cover type formed a notable exception as we used the dominant cover type within each

103   larger 0.25° grid cell.

104   **Savanna and grassland cover.** We used the Moderate Resolution Imaging

105   Spectroradiometer (MODIS) Global Land Cover product (MCD12C1 collection 5.1) for 2012

106   (Friedl *et al.*, 2010) to delimit savanna and grassland extent across continents. We included all

107   0.25° grid cells (25°N - 25°S) where savannas and grasslands formed the dominant land cover

108   type, based on the combined cover of "woody savannas", "savannas", and "grasslands"

109   according to the International Geosphere-Biosphere Programme (IGBP) classification. We

110   focus on "natural lands", by excluding croplands and urban areas from our analysis, because

111   we expect that fuel-build up and moisture status would primarily depend on management

112   practice instead of antecedent rainfall across these landscapes. In addition, we used the

113   MODIS vegetation continuous fields product (MOD44B collection 5 for 2010, (DiMiceli *et*

114   *al.*, 2011) to exclude areas with tree cover > 40%, assuming that savannas with high tree

115   cover are less flammable (Archibald *et al.*, 2009), and because fires are difficult to detect

116   under canopies (Morton *et al.*, 2011). In this study we analyzed data from Africa (55.6%),

117   Australia (7.8%) and South America (27.4%), together containing 90.8% of the delimited

118   tropical savannas and grasslands. Tropical savannas in Asia (6.1%) and Central America

119   (3.1%) are highly fragmented and poorly defined (e.g., Ratnam *et al.*, 2016), and were

120   therefore excluded from our analysis.

121   **Burned area data.** We derived the percentage of monthly burned area per 0.25° grid cell

122   from the MODIS MCD64A1 collection 6 global burned area product (Giglio *et al.*, 2018).

123   Subsequently, we derived time series of annual burned area (BA in % yr^{-1}) per fire year for

124   each 0.25° grid cell for 2002–2016. For each grid cell, we delimited the fire-year as the 12-

125   month period centered on the month of maximum mean burned area (from 5 months before to

126   6 months after the month of maximum burned area). This step is required because in the

127   northern hemisphere tropics the fire season typically includes months of two calendar years,

128   with maximum fire activity occurring in December or January. Based on these fire years, we

129   defined the start and end months of the burning season as the all-year mean month where 10%

130   and 90% of annual burned area had occurred, respectively. Our analysis is based on the

131   assumption of clear seasonality with a unique fire season per year, which is generally true

132   across tropical grasslands and savannas (Benali *et al.*, 2017).

Burned area drivers. Monthly rainfall data were obtained from the Climate Hazards Group InfraRed Precipitation with Station (CHIRPS) dataset (Funk *et al.*, 2015) for the extended study period between 2002–2016. We used rainfall data to calculate mean annual rainfall (MAR, in mm yr^{-1}, Fig 1b) over the calendar year and estimate the *fuel moisture* and *fuel build-up effects* on interannual variability in burned area. We defined the *fuel moisture effect* as the accumulated rainfall during the six months prior to the end of the burning season. We assumed that rainfall occurring during, or just before the burning season determines the probability of ignition and fire spread. The *fuel build-up effect* was defined as the accumulated rainfall during 24 months prior to the end of the burning season, as previous rainfall is an important control on the amount of biomass produced. We selected the 6- and 24-months cut-off as, on average, the strongest negative response in *fuel moisture limited* landscapes was found around 6-7 months of antecedent rainfall (Fig. A1), while across *fuel build-up limited* landscapes accumulated rainfall over two wet seasons (24-months) had a slightly higher explanatory power than over a single wet season (12-months) (Fig. A1).

We considered three explanatory variables for our initial analysis of the drivers of observed spatial patterns in *fuel build-up* and *fuel moisture limited* fire regimes. First, we focus on spatial differences in dry season duration. Following Hulme & Viner (1998), we define the dry season duration (in months) as the average number of months with rainfall below 50 mm month^{-1} during the 2002 – 2016 calendar years (Fig. A2b). This intermediate (50 mm month^{-1}) rainfall threshold assures reasonable sensitivity to dry season duration across both arid and more humid tropical environments. Second, to investigate how humans affect fire occurrence and climate-fire interactions, we used the Wildlife and Conservation Society (WCS) Human Influence Index (HII, Fig. A2a) (WCS & University, 2005), a measure, varying between 0 and 64 (for no human and maximum influence respectively), of the direct human influence on ecosystems based on eight different measures of human presence: population density (people per km^2), land cover type, and a measure of the presence of railroads, major roads, navigable rivers, coastlines, nighttime stable lights, and urban polygons. Third, because vegetation structure can affect fire activity and varies across continents (Lasslop *et al.*, 2018), we also considered tree cover as an explanatory variable for observed patterns of *fuel* and *moisture limited* fire regimes. Tree cover data was obtained from MODIS vegetation continuous fields (MOD44B collection 5, Fig. A2c) for 2010 (DiMiceli et al., 2011). Because in our definition of tropical savannas and grasslands we already excluded areas with tree cover >40%, this variable ranged from 0 to 40%.

2.2. Methods

Burned area response to *fuel moisture* and *fuel build-up effects*. Based on the per-fire-year

burned area time series, we explored the response of annual burned area to interannual

variability in rainfall for each 0.25° grid cell. All grid cells that showed negative correlations

(Pearson's r) between antecedent rainfall accumulated over 6 months prior to the end of the

burning season and annual BA were considered *fuel moisture limited* fire regimes, indicating

higher burned area when accumulated rainfall was low during or shortly before the burning

season. Similarly, we considered ecosystems to be *fuel build-up limited*, for all grid cells with

a positive correlation between annual BA and antecedent rainfall accumulated during 24

months prior to the end of the burning season. Some grid cells had both negative correlations

(*fuel moisture effect*) with the short lead times and positive correlations (*fuel build-up effect*)

with the long lead times, but in these cases, effects were generally not significant at the same

time ($p<0.05$ in 5% of total grid cells). For simplicity, we therefore selected the strongest

absolute correlation for each grid cell.

Based on the biome wide characterization of burned area response to antecedent rainfall,

we explored how these relationships varied across continents. First, we identified the MAR

threshold where fire regimes switched from being *fuel build-up limited* to being *fuel moisture*

limited. We binned the per grid cell strongest absolute (i.e. positive or negative) correlation

between annual BA and antecedent rainfall into 100 mm MAR bins. We then defined the

threshold where ecosystems switched from *fuel build-up limited* to *fuel moisture limited* (and

vice versa) as the MAR bin where >50% of the correlation coefficients switched from

negative to positive (i.e. the median value in a boxplot crossed the zero line).

Drivers of burned area response. We used two different approaches to explore the drivers

of spatial differences in the relationship between annual burned area and antecedent rainfall.

First, to keep annual rainfall constant, we binned all grid cells based on 200 mm yr^{-1} MAR

increments; within each rainfall bin, we further subdivided the grid cells based on bins of dry

season duration (DS; increments of months with rainfall below 50 mm), Human Influence

Index (HII; increments of 5 units of HII, HII ranged from 0 to 40 across the study area), and

tree cover (TC; 5% increments from 0 to 40%). Based on this subdivision along rainfall

gradients, we explored how DS, HII, and TC modified patterns of a) mean annual burned

area, b) interannual variability in burned area (measured as the coefficient of variation), and c)

the correlation coefficient between antecedent rainfall and annual BA.

198   Second, we compared two multiple linear regression models to understand how the *fuel*
199   *moisture effect* (Rain6, 6 months of accumulated rainfall) and the *fuel build-up effect* (Rain24,
200   24 months of accumulated rainfall) influenced the interannual variability of BA (Eq. 1) and
201   investigate if BA response to rainfall varied at continental scales (Eq. 2). In order to increase
202   model sensitivity to temporal variability in burned area, we used burned area anomalies rather
203   than absolute burned area time series.

204

205            $BA_{i,j}$ anomaly $\sim \alpha + \beta_1 * Rain6_{i,j} + \beta_2 * Rain24_{i,j} + \varepsilon$ Equation 1
206       $BA_{i,j}$ anomaly $\sim \alpha + \beta_1 * Rain6_{i,j} : Continent + \beta_2 * Rain24_{i,j,t} : Continent + \varepsilon$ Equation 2

207   where $BA_{i,j}$ anomaly is the burned area anomaly for each pixel (i) and year (j) calculated as
208    $BA_{i,j}$ – mean BA_i, β parameters represent the slope of the linear regression between the BA
209   anomaly and the explanatory variables ($Rain6_{i,j}$ and $Rain24_{i,j}$), α is the intercept and ε the
210   residual error term. The BA anomaly includes both negative and positive values, where
211   negative values indicate that the BA for the year *j* was lower than the mean BA and positive
212   values indicate that annual BA was higher than the mean. Thus, β_1 and β_2 indicate the rate of
213   BA change per unit of accumulated rainfall (% year^{-1} mm^{-1}).

214   Next, we explored how other variables, including MAR, DS, HII and/or TC modify the
215   influence of antecedent rainfall on burned area anomalies by analyzing how the β_1 and β_2
216   values changed when introducing each driver in the model. In addition, when including a new
217   variable, we compared the model with and without the effect in question, using an ANOVA
218   likelihood-ratio test and AIC (Akaike's Information Criterion) to confirm the selection of the
219   best model (Burnham & Anderson, 2004). Finally, we constructed the same models, but now
220   based on full burned area time series instead of anomalies. This analysis helped to understand
221   how each variable contributes to both spatial and temporal patterns of biome wide burned
222   area. All analyses were done using the 'raster' and 'rgdal' packages in R, version R2.5.1 (R
223   Core Team, 2016).

224   **3.   Results**
225   **3.1. Burned area response to antecedent rainfall**

226   We observed the strongest correlations between antecedent rainfall and annual burned area
227   (BA) in frequently burning savannas and grasslands across the tropics (Fig. 1). Here we
228   considered grid cells with a negative correlation between burned area and rainfall (6-month
229   lead time) to be *fuel moisture limited* and grid cells with a positive correlation (24-month lead

230 time) to be *fuel build-up limited*. Interestingly, we found that savannas with *fuel build-up*
231 *limited* fire regimes (41.4%) in more arid regions covered less area than savannas with *fuel*
232 *moisture limited* fire regimes (58.6%, Fig. 1b, e) in more humid systems. Mean annual rainfall
233 (MAR) varied widely across tropical savannas on the three continents, resulting in
234 predominantly *fuel moisture limited* fire regimes across the relatively humid savannas of
235 South America, and *fuel build-up limited* fire regimes across Australian savannas that were
236 more arid on average (Fig. 1b to 1e). Africa showed a mix of *fuel* and *moisture limited*
237 savannas across a large rainfall gradient. For example, we observed strong positive
238 correlations for arid regions (e.g. Namibia, Botswana and Zimbabwe) and strong negative
239 correlations for humid regions (e.g. the north of Mozambique and the south of Tanzania and
240 the Democratic Republic of Congo) (Fig. 1e).

241 **3.2. Continental differences in the switch from fuel build-up to fuel moisture**
242   **limitation**

243   Africa tropical savanna and grassland fire regimes switched from a predominantly positive
244 (*fuel build-up effect*) to negative (*fuel moisture effect*) response to antecedent rainfall around
245 800 mm annual rainfall (Fig. 2), while fire regimes in South America switched around 500
246 mm yr^{-1}, and in Australia around 1000 mm yr^{-1} (Fig. 2). For all three continents, MAR bins
247 that contained a low number of grid cells often showed a more variable response (cf. Figs. 2
248 and A3). We also observed large spatial variability in burned area-rainfall responses (Fig. 1
249 and 2), indicating that the switch from *fuel build-up* to *fuel moisture limited* fire regimes
250 occurred gradually. On each continent, there was a transition zone in MAR levels rather than
251 a clear threshold, where the strength of the dominant correlation weakened before switching
252 to a different dominant driver. Only 24% of South American savannas were *fuel build-up*
253 *limited* against 61% of Australian savannas and 47% of African savannas.

254 **3.3.Drivers of continental differences.**

255   In addition to MAR, we explored how rainfall seasonality influences median annual BA
256 and interannual variability in BA, both important indicators of the strength of fire-climate
257 interactions. Globally, longer dry season durations tended to increase median annual BA,
258 particularly in intermediate productive savannas and grasslands (MAR between 900-1500
259 mm, Fig 3a). Interestingly, when dry season length exceeded 9 months, annual burned area
260 typically declined again, likely because very short growing seasons may limit ecosystem
261 productivity and thus fuel availability. In addition to burned area, we also analyzed its
262 coefficient of variation, we hypothesize that the strength of the burned area response to

263 antecedent rainfall partly depends on the variability of both variables. For bins of comparable
264 rainfall and dry season duration, Australia showed the lowest coefficients of variation,
265 potentially weakening correlation coefficients between antecedent rainfall and burned area,
266 seen as a more variable response of positive and negative correlations (Fig 3b and c). In
267 contrast, large on average coefficients of variation across South America may be responsible
268 for the relatively strong negative correlation observed across productive savannas. We also
269 observed a reduction in the coefficient of variation in areas of high fraction of annual burned
270 area (Fig. 3b), possibly reducing the strength of the correlation between annual burned area
271 and fuel conditions (Fig. 3c). Although dry season duration clearly affected burned area and
272 it's variability, patterns were not uniform, suggesting other factors also played a role.

273 Human impact strongly reduced burned area across continents (Fig. 4a), while Australian
274 savannas and grasslands were generally characterized by low human impact values (HII <10)
275 and African and South American savannas were characterized by higher impact values (HII =
276 10-25; Fig. 4b). The coefficient of variation was clearly reduced in natural areas with a large
277 fraction of burned area and low human influence (Fig. 4b). Despite the large impact of HII on
278 absolute burned area, impacts on the interannual variability were more limited and complex.
279 Globally, a small decline in the strength of the burned area response to rainfall variability was
280 observed with decreasing HII and increasing burned area in the peak biomass burning regions
281 (MAR ranging from 900 – 1500 mm yr^{-1}; Fig. 4c). In contrast, at continental scales sometimes
282 the opposite pattern was observed. For example, in productive savannas (MAR 1300 – 2100
283 mm yr^{-1}) of South America the negative correlation between antecedent rainfall and burned
284 area strengthened with decreasing HII. The global pattern in the response of BA to the *fuel*
285 *build-up* and *fuel moisture effects* was mainly determined by South America and Africa, with
286 a dominant negative response in savannas with MAR above 900 mm yr^{-1} and positive
287 response in savannas with MAR below 900 mm yr^{-1}, independently of the HII (Fig. 4c).

288 Vegetation structure also influenced biome wide patterns of burned area and the strength
289 and sign of correlation coefficients between antecedent rainfall and burned area (Fig. 5). As
290 expected, we observed that higher tree cover was often associated with reduced burned area,
291 particularly in the humid tropics (Fig. 5a). In productive savannas (MAR ranging from 900 to
292 2000 mm yr-1), the fuel moisture effect tended to strengthen with increasing tree cover,
293 although relationships were often weak (Fig. 5c). In fuel limited ecosystems of Australia,
294 there was a weak increase in the strength of the fuel build-up effect with tree cover, opposite
295 to the global pattern, where the strength of the fuel build-up effect weakened with increasing

296   tree cover. As noted earlier, coefficients of variation varied widely across continents, possibly

297   strengthening or weakening regional correlation coefficients. In contrast to Africa and

298   Australia, South America showed high coefficients of variation for savannas of intermediate

299   productivity, likely contributing to the exceptionally strong moisture limitation on regional

300   burned area.

301   Despite the clear biome wide patterns of *fuel moisture* and *fuel build-up limited* fire

302   regimes, we could not establish a single global model to explain the interannual variability in

303   burned area (BA) based on *fuel build-up effect* and *fuel moisture effect* alone (Table 1). Here

304   we used multiple linear regression models to test the effect of the antecedent rainfall on BA

305   anomalies (Table 1) per pixel across the time series, and the spatial and temporal pattern in

306   BA time series (Table A1), across tropical savannas and grasslands. We expect that the model

307   based on BA anomalies is better able to capture interannual variability, while the second

308   model captures both temporal variability and spatial patterns of burned area. The global

309   model of BA anomalies that included only the *fuel build-up effect* and *fuel moisture effect* as

310   explanatory variables explained less than 1% of BA variation (Table 1), while the same model

311   for absolute BA explained 3% of the variance (Table A1). Surprisingly, BA did not vary as

312   expected when an interaction term between MAR and *fuel build-up effect* and *fuel moisture*

313   *effect* was added to the model and its performance did not improve. In contrast, the inclusion

314   of "continent" as an interaction term with the 6- and 24-month accumulated rainfall increased

315   the percent of explained variance and reduced AIC for both BA (from 3.6 to 19%, Table A1)

316   and its internannual variability (from 0.0019 to 0.0029%, Table1). Both models, supported

317   different slopes between the *fuel moisture effect* and *fuel build-up effect* and burned area

318   across continents (p < 0.001), confirming continental scale differences in burned area-rainfall

319   response (Table 1 and A1, Fig. 2).

320   The models with the highest explanatory power (lowest AIC) explained 0.4% of the

321   variance of the interannual variability of BA (Table 1) and 29% of spatial occurrence (Table

322   A1). These models included *tree cover*, *dry season duration* and *HII* all in interaction with

323   *Continent* as additional factors to *fuel build-up effect* and *fuel moisture effect.* The response of

324   BA anomalies to the *fuel-moisture effect* and the *fuel build-up effect* was strongest in Australia

325   (β_1 = -0.0036 % mm^{-1} and β_2 = 0.0019 % mm^{-1} respectively, Table 1) and weakest in Africa

326   (β_1 = -0.0012 % mm^{-1} and β_2 =0.00035 % mm^{-1} respectively, Table 1). Statistical analysis

327   confirmed the expected response, with negative slope coefficients for *fuel moisture effect* and

328   positive coefficients for *fuel build-up effect* (Table 1). The inclusion of *tree cover*, *dry season*

329 *duration* or *HII* in the models modified the slopes of *fuel build-up effect* across all the three
330 continents, while the slopes for *fuel moisture effect* remained more similar (Table 1). When
331 we included all three variables in the model, we detected a slight decrease in the slope of *fuel*
332 *build-up effect* for African (from 0.00041 to 0.00035% mm^{-1}) and South America savannas
333 (from 0.00058 to 0.00046% mm^{-1}) and a larger increase for Australian savannas (from
334 0.00088 to 0.0019% mm^{-1}, Table 1). The inclusion of these three factors also modified the
335 intercept sign from negative to positive indicating a positive anomaly (BA > mean BA) when
336 these factors are zero. When considering the inclusion of each of these explanatory variables
337 (DS, HII, and TC) separately, the inclusion of dry seasons length had the strongest effect on
338 the response of BA to the *fuel build-up effect;* in Africa β_2 decreased from 0.00041 to
339 0.00023% mm^{-1} and the smallest effect was observed in South America from 0.00058 to
340 0.00051 % mm^{-1}. In contrast, the inclusion of HII had the strongest effect on the response of
341 BA to the *fuel build-up effect* in Australia β_2, increasing from 0.00088 to 0.0011% mm^{-1} while
342 in Africa and South America we observed a slight decrease (from 0.00041 to 0.00040% mm^{-1}
343 and from 0.00058 to 0.00054% mm^{-1} respectively). The inclusion of tree cover had the
344 strongest effect on the response of BA to the *fuel build-up effect* for South America, β_2
345 increased from 0.00058 to 0.010% mm^{-}1. When we analyzed the absolute BA (Table A1), HII
346 coefficients were also negative for the three continents, in line with lower burned area in
347 human dominated landscapes (Archibald *et al.*, 2012; Andela *et al.*, 2017), with the highest
348 decrease in BA variation when human influence increased in Australia (β_4 = -3.10%), and a
349 similar lower variation observed in Africa and South America (β_4 = -1.29% and -1.10%
350 respectively, Table A1).
351
352 **4. Discussion**
353 **4.1. Fire-climate threshold**

354   Here we explore the extent of *fuel build-up* and *fuel moisture limited* fire regimes across
355 tropical savannas based on a per-pixel temporal correlation between burned area and
356 antecedent rainfall. Savanna fire-climate interactions changed along gradients of mean annual
357 precipitation, with burned area in xeric savannas being primarily limited by fuel build-up and
358 in mesic savannas by fuel moisture (Fig. 1, Krawchuk & Moritz, 2011; Kahiu & Hanan,
359 2018). In line with previous work, we find that fire activity in humid savannas and grasslands
360 primarily responds to drought conditions during the fire season (Archibald *et al.*, 2010;
361 Lehsten *et al.*, 2010; Alvarado *et al.*, 2017) similar to tropical rainforests (Aragão *et al.*,

362   2008). We find that fuel moisture was the dominant control on fire activity over 58.6% of
363   tropical savannas and grasslands. These systems currently account for 59.1% of the tropical
364   area burned, and the remaining 40.9% is in systems are fuel build-up limited.

365   Striking differences were observed across continents, with large areas of *fuel build-up*
366   *limited* fire regimes occurring across more arid grasslands and savannas of southern Africa
367   and northern Australia, and a near-absence of *fuel build-up limited* systems in tropical South
368   America (Figs. 1 and 2). Fuel moisture formed the key control on burned area across South
369   America's savannas, except for more arid grasslands along the eastern edge of the Brazilian
370   Cerrado. Burned area in arid regions of Africa and Australia responded strongly to antecedent
371   rainfall, highlighting the importance of fuel build-up and connectivity in these regions
372   (Archibald *et al.*, 2010; Whitlock *et al.*, 2010; Krawchuk & Moritz, 2011; Price *et al.*, 2015).
373   Continental scale differences were partly driven by differences in climate, for example, the
374   extent of semi-arid and arid savannas with MAR<1000 mm yr-1 was largest across Africa and
375   Australia, resulting in an overall larger fraction of ecosystems where fire occurrence was
376   limited by *fuel build-up* (Fig. 1; Archibald *et al.*, 2010a). However, savanna fire regimes also
377   switched from being dominantly *fuel build-up limited* to *fuel moisture limited* at different
378   thresholds, around 500 mm yr^{-1} in South America, 800 mm yr^{-1} in Africa, and 1000 mm yr^{-1}
379   in Australia (Fig. 2). Together, these two factors resulted in continental scale differences in
380   fire regimes, and fire activity was limited by *fuel build-up* in only 24% of South American
381   savannas, against 47% of African savannas and 61% of Australian savannas. Interestingly,
382   these continental differences in fire regimes are in line with previous work showing similar
383   differences in controls on savanna distribution and structure (Lehmann *et al.*, 2011, 2014). In
384   the transition zones, where fire regimes switched from being predominantly *fuel-build up*
385   *limited* to *fuel moisture limited*, the relationship between burned area and fuel dryness or fuel
386   availability was often weak, and likely further modified by other climatic, ecological, and
387   anthropogenic factors influencing fuel conditions.

388   **4.2. Drivers of fire response**

389   Seasonal rainfall distribution varied considerably across continents and had a strong effect on
390   annual burned area (Fig. 3a). Previous analyses have shown that rainfall amount during the
391   dry and wet seasons contribute to explain the spatial patterns of tropical fire activity (van der
392   Werf *et al.*, 2008; Bowman *et al.*, 2014; Chen *et al.*, 2017), and that climate seasonality can
393   explain observed differences in fire activity across regions with similar MAR (Saha *et al.*,
394   2019). We found that a minimum dry season duration of 6 to 8-months was required for

395   frequent fires to occur in productive and humid savannas, but we only detected a weak
396   relationship between annual burned area and increasing dry season lengths longer than six
397   months. A possible explanation for this weak relationship could be that dry season duration
398   longer than six months may limit herbaceous productivity by shortening the growing season
399   in spite of MAR. In addition, our results suggest that observed differences in rainfall
400   seasonality may also modify the response of burned area to antecedent rainfall across different
401   regions (Fig. 3b and c). Although the relatively long and pronounced African dry season is
402   one of the factors contributing to high fire frequencies across the continent (Archibald *et al.*,
403   2009), African savannas were characterized by relatively low variability in burned area. In
404   contrast, South American savannas were characterized by lower fire frequencies, but showed
405   higher interannual variability in burned area driven by climate anomalies (cf. Figs. 3b and c;
406   Alvarado *et al.*, 2017b; Chen *et al.*, 2017; Mataveli *et al.*, 2018).

407   Several analyses have shown that human land management, and therefore population
408   density has a significant impact on global burned area (Bistinas *et al.*, 2013). In line with
409   these findings, we found that higher human influence significantly reduced burned area across
410   continents, with larger consequences for more densely populated continents like Africa and
411   South America compared to Australia (Fig. 4a and Table A1; Archibald *et al.*, 2012; Andela
412   *et al.*, 2017). Previous work has also shown that human land management may reduce the
413   sensitivity of fire regimes to climate extremes (Bird et al., 2016). We found that the observed
414   biogeographic differences in fire responses to antecedent rainfall could be related to human
415   land management to some extent, but this factor alone could not explain the differences
416   observed across continents (Fig. 4c). In general, areas with large annual mean burned area and
417   low population densities, showed a relatively strong burned area response to rainfall
418   variability. Nevertheless, this pattern did not hold everywhere, and particularly in savannas of
419   intermediate productivity we observed an overall increase in the strength of the fuel-moisture
420   effect on burned area in human dominated landscapes.

421   Continental scale differences in tree cover also explained part of the observed differences
422   in fire-climate interactions. Previous work has shown that tree cover may limit fire activity in
423   savannas (Archibald *et al.*, 2009), though these effects may be partly masked out in our study,
424   that focuses on more open cover types with tree cover smaller or equal to 40%. Across areas
425   with *fuel moisture limited* fire regimes, we observed a slight increase in the strength of the
426   responses of BA to the antecedent rainfall with the increase of tree cover at similar MAR.
427   While all three variables (DS, HII and TC) modified the response of burned area to antecedent

428 rainfall, none of these variables could explain the differences in thresholds observed across
429 the continents (Figs. 3, 4 and 5). For example, when controlling for TC, continental scale
430 differences in rainfall thresholds at which savannas switched from *fuel build-up* to *fuel*
431 *moisture limited* fire regimes remained different.

432   To confirm these findings, we used a range of multiple linear regression models to explore
433 if the continental scale differences could be explained by differences in DS, HII, and TC.
434 Allowing the burned area to respond differently to antecedent rainfall across continents
435 caused a considerable model improvement both when modeling absolute burned area (Table
436 A1) or it's variability (Table 1). While the introduction of DS, HII and TC as additional
437 explanatory variables further improved model performance, they only marginally affected
438 continental scale differences in burned area response to antecedent rainfall (compare slopes in
439 Table 1). Nevertheless, our linear model explained just 29% of absolute burned area and
440 about 1% of the burned area anomalies even when considering continental scale differences in
441 DS, HII and TC as additional drivers. Improving model representation of fire response to
442 antecedent rainfall therefore remains a topic of future investigation. While we explored the
443 role of dry season duration, it is possible that other indicators of vegetation and fuel
444 conditions, like evapotranspiration, also play an important role (Boer et al. 2016). Similarly,
445 regional differences in herbivory and human fire management, as well as the different
446 composition and structure of grass and tree communities across continents may also be
447 important (Lehmann et al., 2011).

448   Understanding the distribution of *fuel build-up* - and *fuel moisture limited* fire regimes is
449 critical for fire management now and in the future, as changes in land management or climate
450 may result in contrasting responses across *fuel* and *moisture limited* systems. In contrast to
451 earlier studies that have suggested that fire activity in savannas was mostly limited by fuel
452 availability (Whitlock *et al.*, 2010; Krawchuk & Moritz, 2011), we found that fuel moisture
453 controlled burned area variability in more than half (58.6%) of the tropical savannas and
454 grasslands, accounting for 59,1% of total burned area. Striking differences in burned area
455 response to rainfall variability across continents highlighted that South American savannas
456 were particularly sensitive to fuel moisture conditions, suggesting that rising temperatures
457 may increase fire activity across the continent, and explaining the extraordinary strong
458 response of fire activity across the continent to drought conditions driven by sea surface
459 temperature anomalies (Chen et al., 2011). In contrast, a reduction of moisture availability
460 would likely decrease burned area over most of Australia, where fire activity was mainly
461 controlled by fuel build-up. In African savannas and grasslands, the area where burned area

462 was primarily controlled by fuel build-up was about equal to the area where fuel moisture
463 conditions were most important. Although we could not conclusively attribute the continental
464 scale differences to a single driver, we found that rainfall seasonality, human land
465 management and tree cover all modified fire-climate interactions regionally through their
466 effects on fuel availability and moisture status. Our work demonstrates that one single "global
467 model" for savanna fires will not be enough to predict future fire regimes and fire regimes
468 across different continents will likely respond differently to the same drivers of global change.
469

References

471 Abatzoglou, J.T., Williams, A.P., Boschetti, L., Zubkova, M. & Kolden, C.A. (2018) Global patterns of
472   interannual climate-fire relationships. *Global Change Biology*, **24**, 5164–5175.

473 Aleman, J.C. & Staver, A.C. (2018) Spatial patterns in the global distributions of savanna and forest. *Global*
474   *Ecology and Biogeography*, **27**, 792–803.

475 Alvarado, S.T., Fornazari, T., Cóstola, A., Morellato, L.P.C. & Silva, T.S.F. (2017) Drivers of fire occurrence in
476   a mountainous Brazilian cerrado savanna: Tracking long-term fire regimes using remote sensing.
477   *Ecological Indicators*, **78**, 270–281.

478 Andela, N., Morton, D.C., Giglio, L., Chen, Y., van der Werf, G.R., Kasibhatla, P.S., DeFries, R.S., Collatz,
479   G.J., Hantson, S., Kloster, S., Bachelet, D., Forrest, M., Lasslop, G., Li, F., Mangeon, S., Melton, J.R.,
480   Yue, C. & Randerson, J.T. (2017) A human-driven decline in global burned area. *Science*, **356**, 1356–
481   1362.

482 Aragão, L.E.O.C., Malhi, Y., Barbier, N., Lima, A., Shimabukuro, Y., Anderson, L. & Saatchi, S. (2008)
483   Interactions between rainfall, deforestation and fires during recent years in the Brazilian Amazonia.
484   *Philosophical Transactions of the Royal Society B: Biological Sciences*, **363**, 1779–1785.

485 Archibald, S., Nickless, A., Govender, N., Scholes, R.J. & Lehsten, V. (2010) Climate and the inter-annual
486   variability of fire in southern Africa: a meta-analysis using long-term field data and satellite-derived burnt
487   area data. *Global Ecology and Biogeography*, **19**, 794–809.

488 Archibald, S., Roy, D.P.D., Wilgen, V., Brian, W. & Scholes, R.J. (2009) What limits fire? An examination of
489   drivers of burnt area in Southern Africa. *Global Change Biology*, **15**, 613–630.

490 Archibald, S., Staver, A.C. & Levin, S.A. (2012) Evolution of human-driven fire regimes in Africa. *Proceedings*
491   *of the National Academy of Sciences*, **109**, 847–852.

492 Benali, A., Mota, B., Carvalhais, N., Oom, D., Miller, L.M., Campagnolo, M.L. & Pereira, J.M.C. (2017)
493   Bimodal fire regimes unveil a global-scale anthropogenic fingerprint. *Global Ecology and Biogeography*,
494   **26**, 799–811.

495 Bird, R.B., Bird, D.W. & Codding, B.F. (2016) People, El Niño southern oscillation and fire in Australia: fire
496   regimes and climate controls in hummock grasslands. *Philosophical transactions of the Royal Society of*
497   *London. Series B, Biological sciences*, **371**, 20150343.

498 Bird, R.B., Codding, B.F., Kauhanen, P.G. & Bird, D.W. (2012) Aboriginal hunting buffers climate-driven fire-
499   size variability in Australia's spinifex grasslands. *Proceedings of the National Academy of Sciences of the*
500   *United States of America*, **109**, 10287–10292.

501 Bistinas, I., Harrison, S.P., Prentice, I.C. & Pereira, J.M.C. (2014) Causal relationships versus emergent patterns
502   in the global controls of fire frequency. *Biogeosciences*, **11**, 5087–5101.

503 Bistinas, I., Oom, D., Sá, A.C.L., Harrison, S.P., Prentice, I.C. & Pereira, J.M.C. (2013) Relationships between
504   Human Population Density and Burned Area at Continental and Global Scales. *PLoS ONE*, **8**, e81188.

505 Boer, M.M., Bowman, D.M.J.S., Murphy, B.P., Cary, G.J., Cochrane, M.A., Fensham, R.J., Krawchuk, M.A.,
506   Price, O.F., De Dios, V.R., Williams, R.J. & Bradstock, R.A. (2016) Future changes in climatic water
507   balance determine potential for transformational shifts in Australian fire regimes. *Environmental Research*
508   *Letters*, **11**, 065002.

509 Bond, W.J., Woodward, F.I. & Midgley, G.F. (2005) The global distribution of ecosystems in a world without
510   fire. *New Phytologist*, **165**, 525–538.

511 Bowman, D.M.J.S., Balch, J., Artaxo, P., Bond, W.J., Cochrane, M.A., D'Antonio, C.M., DeFries, R., Johnston,
512   F.H., Keeley, J.E., Krawchuk, M.A., Kull, C.A., Mack, M., Moritz, M.A., Pyne, S., Roos, C.I., Scott, A.C.,
513   Sodhi, N.S. & Swetnam, T.W. (2011) The human dimension of fire regimes on Earth. *Journal of*
514   *Biogeography*, **38**, 2223–2236.

515 Bowman, D.M.J.S., Murphy, B.P., Williamson, G.J. & Cochrane, M.A. (2014) Pyrogeographic models,
516   feedbacks and the future of global fire regimes. *Global Ecology and Biogeography*, **23**, 821–824.

517 Bradstock, R.A. (2010) A biogeographic model of fire regimes in Australia: current and future implications.
518   *Global Ecology and Biogeography*, **19**, 145–158.

519 Burnham, K.P. & Anderson, D.R. (2004) Multimodel Inference Understanding AIC and BIC in Model Selection.
520   *Sociological Methods & Research*, **33**, 261–304.

521 Chen, Y., Morton, D.C., Andela, N., van der Werf, G.R., Giglio, L. & Randerson, J.T. (2017) A pan-tropical
522   cascade of fire driven by El Niño/Southern Oscillation. *Nature Climate Change*, **7**, 906–911.

523 Chen, Y., Randerson, J., Morton, D., DeFries, R., Collatz, G., Kasibhatla, P., Giglio, L., Jin, Y. & Marlier, M.
524   (2011) Forecasting fire season severity in South America using sea surface temperature anomalies.
525   *Science*, **334**, 787–791.

526 Chuvieco, E., Giglio, L. & Justice, C. (2008) Global characterization of fire activity: toward defining fire
527   regimes from Earth observation data. *Global Change Biology*, **14**, 1488–1502.

528 Cochrane, M.A. & Ryan, K.C. (2009) *Fire and fire ecology: Concepts and principles*. Springer Praxis Books.,
529   pp. 25–62. Springer Berlin Heidelberg.

530 Daniau, A.-L., Bartlein, P.J., Harrison, S.P., Prentice, I.C., Brewer, S., Friedlingstein, P., Harrison-Prentice, T.I.,
531   Inoue, J., Izumi, K., Marlon, J.R., Mooney, S., Power, M.J., Stevenson, J., Tinner, W., Andrič, M.,
532   Atanassova, J., Behling, H., Black, M., Blarquez, O., Brown, K.J., Carcaillet, C., Colhoun, E.A.,
533   Colombaroli, D., Davis, B.A.S., D'Costa, D., Dodson, J., Dupont, L., Eshetu, Z., Gavin, D.G., Genries, A.,
534   Haberle, S., Hallett, D.J., Hope, G., Horn, S.P., Kassa, T.G., Katamura, F., Kennedy, L.M., Kershaw, P.,
535   Krivonogov, S., Long, C., Magri, D., Marinova, E., McKenzie, G.M., Moreno, P.I., Moss, P., Neumann,
536   F.H., Norström, E., Paitre, C., Rius, D., Roberts, N., Robinson, G.S., Sasaki, N., Scott, L., Takahara, H.,
537   Terwilliger, V., Thevenon, F., Turner, R., Valsecchi, V.G., Vannière, B., Walsh, M., Williams, N. &
538   Zhang, Y. (2012) Predictability of biomass burning in response to climate changes. *Global*
539   *Biogeochemical Cycles*, **26**, GB4007.

540 DiMiceli, C.M., Carroll, M.L., Sohlberg, R.A., Huang, C., Hansen, M.C. & Townshend, J.R.G. (2011) *Annual*
541   *Global Automated MODIS Vegetation Continuous Fields (MOD44B) at 250 m Spatial Resolution for Data*
542   *Years Beginning Day 65, 2000 - 2010, Collection 5 Percent Tree Cover*, University of Maryland, College
543   Park, MD, USA.

544 Forkel, M., Dorigo, W., Lasslop, G., Teubner, I., Chuvieco, E. & Thonicke, K. (2017) A data-driven approach to
545   identify controls on global fire activity from satellite and climate observations (SOFIA V1). *Geoscientific*
546   *Model Development*, **10**, 4443–4476.

547 Friedl, M.A., Sulla-Menashe, D., Tan, B., Schneider, A., Ramankutty, N., Sibley, A. & Huang, X. (2010)
548   MODIS Collection 5 global land cover: Algorithm refinements and characterization of new datasets.
549   *Remote Sensing of Environment*, **114**, 168–182.

550 Funk, C., Peterson, P., Landsfeld, M., Pedreros, D., Verdin, J., Shukla, S., Husak, G., Rowland, J., Harrison, L.,
551   Hoell, A. & Michaelsen, J. (2015) The climate hazards infrared precipitation with stations—a new
552   environmental record for monitoring extremes. *Scientific Data*, **2**, 150066.

553 Giglio, L., Boschetti, L., Roy, D.P., Humber, M.L. & Justice, C.O. (2018) The Collection 6 MODIS burned area
554   mapping algorithm and product. *Remote Sensing of Environment*, **217**, 72–85.

555 Hantson, S., Arneth, A., Harrison, S.P., Kelley, D.I., Prentice, I.C., Rabin, S.S., Archibald, S., Mouillot, F.,
556   Arnold, S.R., Artaxo, P., Bachelet, D., Ciais, P., Forrest, M., Friedlingstein, P., Hickler, T., Kaplan, J.O.,
557   Kloster, S., Knorr, W., Lasslop, G., Li, F., Mangeon, S., Melton, J.R., Meyn, A., Sitch, S., Spessa, A., van
558   der Werf, G.R., Voulgarakis, A. & Yue, C. (2016) The status and challenge of global fire modelling. **13**,
559   3359–3375.

560 Hantson, S., Scheffer, M., Pueyo, S., Xu, C., Lasslop, G., van Nes, E.H., Holmgren, M. & Mendelsohn, J. (2017)
561   Rare, Intense, Big fires dominate the global tropics under drier conditions. *Scientific Reports*, **7**, 14374.

562 Hoffmann, W.A., Geiger, E.L., Gotsch, S.G., Rossatto, D.R., Silva, L.C.R., Lau, O.L., Haridasan, M. & Franco,
563   A.C. (2012) Ecological thresholds at the savanna-forest boundary: how plant traits, resources and fire
564   govern the distribution of tropical biomes. *Ecology Letters*, **15**, 759–768.

565 Hulme, M. & Viner, D. (1998) *A Climate Change Scenario for the Tropics*. *Potential Impacts of Climate Change*
566   *on Tropical Forest Ecosystems*, pp. 5–36. Springer Netherlands, Dordrecht.

567 Jolly, W.M., Cochrane, M.A., Freeborn, P.H., Holden, Z.A., Brown, T.J., Williamson, G.J. & Bowman, D.M.J.S.
568   (2015) Climate-induced variations in global wildfire danger from 1979 to 2013. *Nature Communications*,
569   **6**, 7537.

570 Kahiu, M.N. & Hanan, N.P. (2018) Fire in sub-Saharan Africa: The fuel, cure and connectivity hypothesis.
571   *Global Ecology and Biogeography*, **27**, 946–957.

572 Krawchuk, M.A. & Moritz, M.A. (2011) Constraints on global fire activity vary across a resource gradient.
573   *Ecology*, **92**, 121–132.

574 Lasslop, G., Moeller, T., D&apos;Onofrio, D., Hantson, S. & Kloster, S. (2018) Tropical climate–
575   vegetation–fire relationships: multivariate evaluation of the land surface model JSBACH. *Biogeosciences*,
576   **15**, 5969–5989.

577 Lehmann, C.E., Anderson, T.M., Sankaran, M., Higgins, S.I., Archibald, S., Hoffmann, W.A., Hanan, N.P.,
578   Williams, R.J., Fensham, R.J., Felfili, J. & others (2014) Savanna vegetation-fire-climate relationships
579   differ among continents. *Science*, **343**, 548–552.

580 Lehmann, C.E.R., Archibald, S.A., Hoffmann, W.A. & Bond, W.J. (2011) Deciphering the distribution of the
581   savanna biome. *New Phytologist*, **191**, 197–209.

582 Lehsten, V., Harmand, P., Palumbo, I. & Arneth, A. (2010) Modelling burned area in Africa. *Biogeosciences*, **7**,
583   3199–3214.

584 van Marle, M.J.E., Kloster, S., Magi, B.I., Marlon, J.R., Daniau, A.-L., Field, R.D., Arneth, A., Forrest, M.,
585   Hantson, S., Kehrwald, N.M., Knorr, W., Lasslop, G., Li, F., Mangeon, S., Yue, C., Kaiser, J.W. & van der
586   Werf, G.R. (2017) Historic global biomass burning emissions based on merging satellite observations with
587   proxies and fire models (1750&amp;ndash;2015). *Geoscientific Model Development Discussions*, **10**,
588   3329–3357.

589 Mataveli, G.A.V., Silva, M.E.S., Pereira, G., Cardozo, F.D.S., Kawakubo, F.S., Bertani, G., Costa, J.C., Ramos,
590   R.D.C. & Silva, V.V. Da (2018) Satellite observations for describing fire patterns and climate-related fire
591   drivers in the Brazilian savannas. *Hazards Earth Syst. Sci*, **18**, 125–144.

592 Mistry, J. (2000) *World savannas: ecology and human use*, Prentice Hall (a Pearson Education Company).

593 Moritz, M.A., Parisien, M.-A., Batllori, E., Krawchuk, M.A., Van Dorn, J., Ganz, D.J. & Hayhoe, K. (2012)
594   Climate change and disruptions to global fire activity. *Ecosphere*, **3**, 1–22.

595 Morton, D.C., DeFries, R.S., Nagol, J., Souza, C.M., Kasischke, E.S., Hurtt, G.C. & Dubayah, R. (2011)
596   Mapping canopy damage from understory fires in Amazon forests using annual time series of Landsat and
597   MODIS data. *Remote Sensing of Environment*, **115**, 1706–1720.

598 O'Donnell, A.J., Boer, M.M., McCaw, W.L. & Grierson, P.F. (2011) Vegetation and landscape connectivity
599   control wildfire intervals in unmanaged semi-arid shrublands and woodlands in Australia. *Journal of*
600   *Biogeography*, **38**, 112–124.

601 Le Page, Y., Oom, D., Silva, J.M.N., Jönsson, P. & Pereira, J.M.C. (2010) Seasonality of vegetation fires as
602   modified by human action: observing the deviation from eco-climatic fire regimes. *Global Ecology and*
603   *Biogeography*, **19**, 575–588.

604 Pausas, J.G. & Paula, S. (2012) Fuel shapes the fire–climate relationship: evidence from Mediterranean
605 ecosystems. *Global Ecology and Biogeography*, **21**, 1074–1082.

606 Pausas, J.G. & Ribeiro, E. (2013) The global fire–productivity relationship. *Global Ecology and Biogeography*,
607 **22**, 728–736.

608 Price, O.F., Pausas, J.G., Govender, N., Flannigan, M., Fernandes, P.M., Brooks, M.L. & Bird, R.B. (2015)
609 Global patterns in fire leverage: The response of annual area burnt to previous fire. *International Journal*
610 *of Wildland Fire*, **24**, 297–306.

611 Price, O.F., Russell-Smith, J. & Watt, F. (2012) The influence of prescribed fire on the extent of wildfire in
612 savanna landscapes of western Arnhem Land, Australia. *International Journal of Wildland Fire*, **21**, 297–
613 305.

614 R Core Team (2016) R: A language and environment for statistical computing. R Foundation for Statistical
615 Computing.

616 Rabin, S.S., Melton, J.R., Lasslop, G., Bachelet, D., Forrest, M., Hantson, S., Kaplan, J.O., Li, F., Mangeon, S.,
617 Ward, D.S., Yue, C., Arora, V.K., Hickler, T., Kloster, S., Knorr, W., Nieradzik, L., Spessa, A., Folberth,
618 G.A., Sheehan, T., Voulgarakis, A., Kelley, D.I., Prentice, I.C., Sitch, S., Harrison, S. & Arneth, A. (2017)
619 The Fire Modeling Intercomparison Project (FireMIP), phase 1: experimental and analytical protocols with
620 detailed model descriptions. *Geoscientific Model Development*, **10**, 1175–1197.

621 Ratnam, J., Tomlinson, K.W., Rasquinha, D.N. & Sankaran, M. (2016) Savannahs of Asia: antiquity,
622 biogeography, and an uncertain future. *Philosophical transactions of the Royal Society of London. Series*
623 *B, Biological sciences*, **371**, 20150305.

624 Saha, M. V., Scanlon, T.M. & D'Odorico, P. (2019) Climate seasonality as an essential predictor of global fire
625 activity. *Global Ecology and Biogeography*, **28**, 198–210.

626 Voulgarakis, A. & Field, R.D. (2015) Fire Influences on Atmospheric Composition, Air Quality and Climate.
627 *Current Pollution Reports*, **1**, 70–81.

628 WCS, W.C.S.- & University, C. for I.E.S.I.N.-C.-C. (2005) Last of the Wild Project, Version 2, 2005 (LWP-2):
629 Global Human Influence Index (HII) Dataset (Geographic).

630 van der Werf, G.R., Randerson, J.T., Giglio, L., Gobron, N. & Dolman, A.J. (2008) Climate controls on the
631 variability of fires in the tropics and subtropics. *Global Biogeochemical Cycles*, **22**, GB3028.

632 Whitlock, C., Higuera, P.E., McWethy, D.B. & Briles, C.E. (2010) Paleoecological perspectives on fire ecology:
633 revisiting the fire-regime concept. *Open Ecology Journal*, **3**, 6–23.

634 Van Wilgen, B.W., Govender, N., Biggs, H.C., Ntsala, D. & Funda, X.N. (2004) Response of Savanna Fire
635 Regimes to Changing Fire-Management Policies in a Large African National Park. *Conservation Biology*,
636 **18**, 1533–1540.

637 Williams, A.P. & Abatzoglou, J.T. (2016) Recent Advances and Remaining Uncertainties in Resolving Past and
638 Future Climate Effects on Global Fire Activity. *Current Climate Change Reports*, **2**, 1–14.

639 Yibarbuk, D., Whitehead, P.J., Russell-Smith, J., Jackson, D., Godjuwa, C., Fisher, A., Cooke, P., Choquenot, D.
640 & Bowman, D.M.J.S. (2002) Fire ecology and Aboriginal land management in central Arnhem Land,
641 northern Australia: a tradition of ecosystem management. *Journal of Biogeography*, **28**, 325–343.

642

643 ## Data Accessibility:

644 Biome wide gridded raster layers (GeoTIFF) of mean annual rainfall, tree cover, dry season duration,
645 and human development index, as well as per fire-year burned area and antecedent rainfall (6 and 24-
646 month accumulation periods) along with inferred maps of fire-response to antecedent rainfall are
647 available on Zenodo web site (https://zenodo.org/)

Tables

Table 1. Multiple Linear Regression Models explaining the variation of annual burned area anomalies ($BA_{i,j}$ *anomaly*) in pixel i and year j for tropical savannas and grasslands areas (2002 – 2016). The variables representing the fuel moisture effect (6 months of accumulated rainfall; $Rain6_{i,j}$), and the fuel build-up effect (24 months of accumulated rainfall; $Rain24_{i,j}$), varied both by pixel i and year j. Other variables, including mean annual rainfall (MAR_i), dry season duration (DS_i), human influence index (HII_i) and tree cover (TC_i) varied by pixel i only. Model performance was evaluated based on the coefficient of determination (R^2), p-value and Akaike's Information Criterion (AIC). All models were significant at $p<0.001$.

| *Regression model*	**Regression equation**	**R^2**	**AIC**
$Rain6_{i,j}$ + $Rain24_{i,j}$	$BA_{i,j}$ anomaly $\sim$ -0.22 – 0.0018 * $Rain6_{i,j}$ + 0.00040 * $Rain24_{i,j}$ + εij	0.0019	2090280
$Rain6_{i,j}$: MAR_i + $Rain24_{i,j}$: MAR_i	$BA_{i,j}$ anomaly $\sim$ 0.0098 – 0.0000011 * $Rain6_{i,j}$: MAR_i + 0.00000018 * $Rain24_{i,j}$: MAR_i + εij	0.0013	2090422
$Rain6_{i,j}$: $Continent_i$ + $Rain24_{i,j}$: $Continent_i$	$BA_{i,j}$ anomaly $\sim$ -0.43 – 0.0011 * $Rain6_{i,j}$: $Africa_i$ – 0.0037 * $Rain6_{i,j}$: $Australia_i$ – 0.0033 * $Rain6_{i,j}$: $SouthAmerica_i$ + 0.00041 * $Rain24_{i,j}$: $Africa_i$ + 0.00088 * $Rain24_{i,j}$: $Australia_i$ + 0.00058 * $Rain24_{i,j}$: $SouthAmerica_i$ + εij	0.0029	2089998
$Rain6_{i,j}$: $Continent_i$ + $Rain24_{i,j}$: $Continent_i$ + DS_i : $Continent$	$BA_{i,j}$ anomaly $\sim$ 0.38 – 0.0012 * $Rain6_{i,j}$: $Africa_i$ – 0.0034 * $Rain6_{i,j}$: $Australia_i$ – 0.0035 * $Rain6_{i,j}$: $SouthAmerica_i$ + 0.00023 * $Rain24_{i,j}$: $Africa_i$ + 0.0014 * $Rain24_{i,j}$: $Australia_i$ + 0.00051* $Rain24_{i,j}$: $SouthAmerica_i$ – 0.062 * DS_i : $Africa_i$ – 0.31 * DS_i : $Australia_i$ – 0.12 * DS_i : $SouthAmerica_i$ + εij	0.0034	2089875
$Rain6_{i,j}$: $Continent_i$ + $Rain24_{i,j}$: $Continent_i$ + HII_i : $Continent_i$	$BA_{i,j}$ anomaly $\sim$ -0.55 – 0.0011 * $Rain6_{i,j}$: $Africa_i$ – 0.0036 * $Rain6_{i,j}$: $Australia_i$ – 0.0033 * $Rain6_{i,j}$: $SouthAmerica_i$ + 0.00040 * $Rain24_{i,j}$: $Africa_i$ + 0.0011 * $Rain24_{i,j}$: $Australia_i$ + 0.00054 * $Rain24_{i,j}$: $SouthAmerica_i$ + 0.011 * HII_i : $Africa_i$ – 0.11 * HII_i : $Australia_i$ + 0.017 * HII_i : $SouthAmerica_i$ + εij	0.0031	2089957
$Rain6_{i,j}$: $Continent_i$ + $Rain24_{i,j}$: $Continent_i$ + TC_i : $Continent_i$	$BA_{i,j}$ anomaly $\sim$ -0.42 – 0.0012 * $Rain6_{i,j}$: $Africa_i$ – 0.0038 * $Rain6_{i,j}$: $Australia_i$ – 0.0033 * $Rain6_{i,j}$: $SouthAmerica_i$ + 0.00049 * $Rain24_{i,j}$: $Africa_i$ + 0.0015 * $Rain24_{i,j}$: $Australia_i$ + 0.00050 * $Rain24_{i,j}$: $SouthAmerica_i$ – 0.010 * TC_i : $Africa_i$ – 0.13 * TC_i : $Australia_i$ + 0.010 * TC_i : $SouthAmerica_i$ + εij	0.0034	2089868
$Rain6_{i,j}$: $Continent_i$ + $Rain24_{i,j}$: $Continent_i$ + TC_i : $Continent_i$ + DS_i : $Continent_i$ + HII_i : $Continent_i$	$BA_{i,j}$ anomaly $\sim$ 0.36 – 0.0012 * $Rain6_{i,j}$: $Africa_i$ – 0.0036 * $Rain6_{i,j}$: $Australia_i$ – 0.0036 * $Rain6_{i,j}$: $SouthAmerica_i$ + 0.00035 * $Rain24_{i,j}$: $Africa_i$ + 0.0019 * $Rain24_{i,j}$: $Australia_i$ + 0.00046 * $Rain24_{i,j}$: $SouthAmerica_i$ – 0.013 * TC_i : $Africa_i$ – 0.13 * TC_i : $Australia_i$ + 0.0077 * TC_i : $SouthAmerica_i$ – 0.055 * DS_i : $Africa_i$ – 0.29 * DS_i : $Australia_i$ – 0.16 * DS_i : $SouthAmerica_i$ – 0.0064 * HII_i : $Africa_i$ + 0.058 * HII_i : $Australia_i$ + 0.016 * HII_i : $SouthAmerica_i$ + εij	0.0039	2089756

Figures
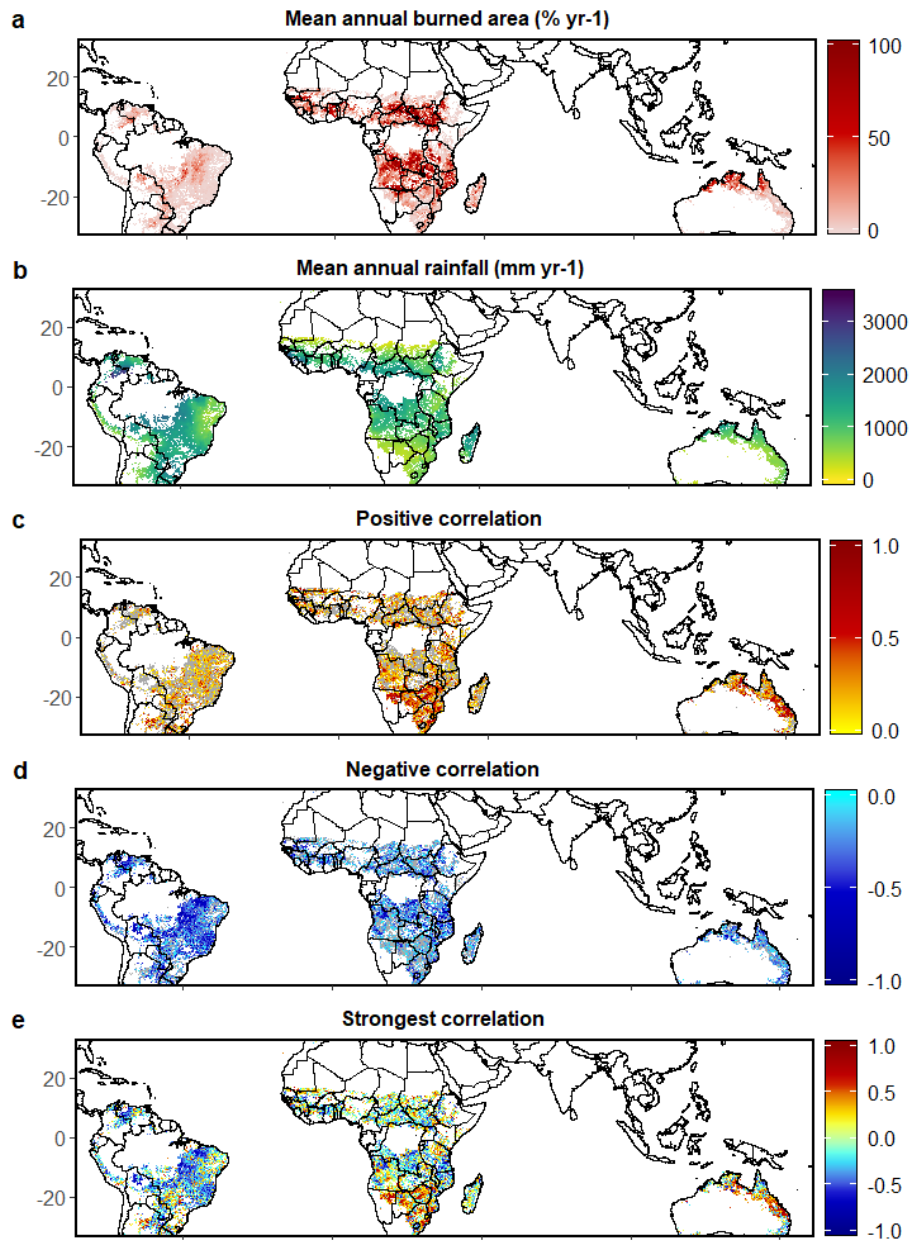
Fig. 1. Rainfall – burned area interactions varied widely across continents. (a) Mean annual burned area (% yr^{-1}), (b) mean annual rainfall (mm yr-1), (c) correlation between annual burned area and 24 months of antecedent rainfall (positive correlations), (d) correlation between annual burned area and 6 months of antecedent rainfall (negative correlations), and (e) the strongest absolute correlation shown in (c and d). Figure e shows the distribution of *fuel build-up limited* (positive correlation) and *fuel moisture limited* (negative correlation) fire regimes across tropical savannas. Grid cells with land cover classes other than savannas and grasslands were excluded from our analysis and are masked in white. Pixels with negative correlations in b and positive correlations in c were masked in grey.

675

676
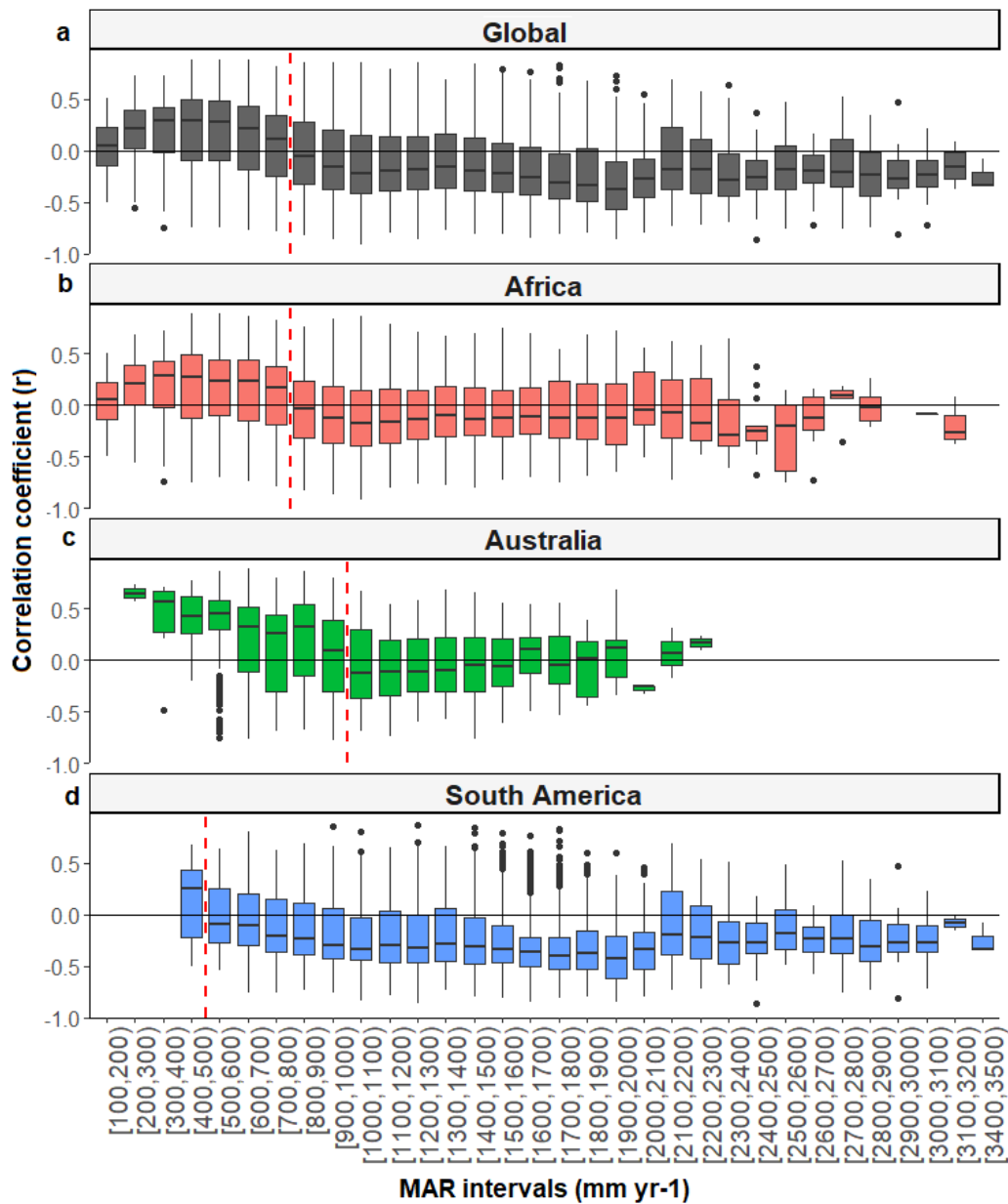
Fig. 2. Box-and-whisker plots of the response of burned area to antecedent rainfall. Results for (a) Pantropical savannas and grasslands, and for (b) Africa, (c) Australia, and (d) South America, separately. Box plots include all 0.25° grid cells per bin of 100 mm mean annual rainfall (MAR). For each grid cell we registered a single response (positive, based on 24-months of antecedent precipitation) or negative (based on 6 months of antecedent rainfall) using the per-grid cell strongest absolute correlation. The boxes indicate the 25th and 75th percentile of the data, the mid band indicates the median, and the whiskers indicate the 5th and 95th percentiles. Box plots with less than 5 pixels were excluded from this figure.

687

688

689

690
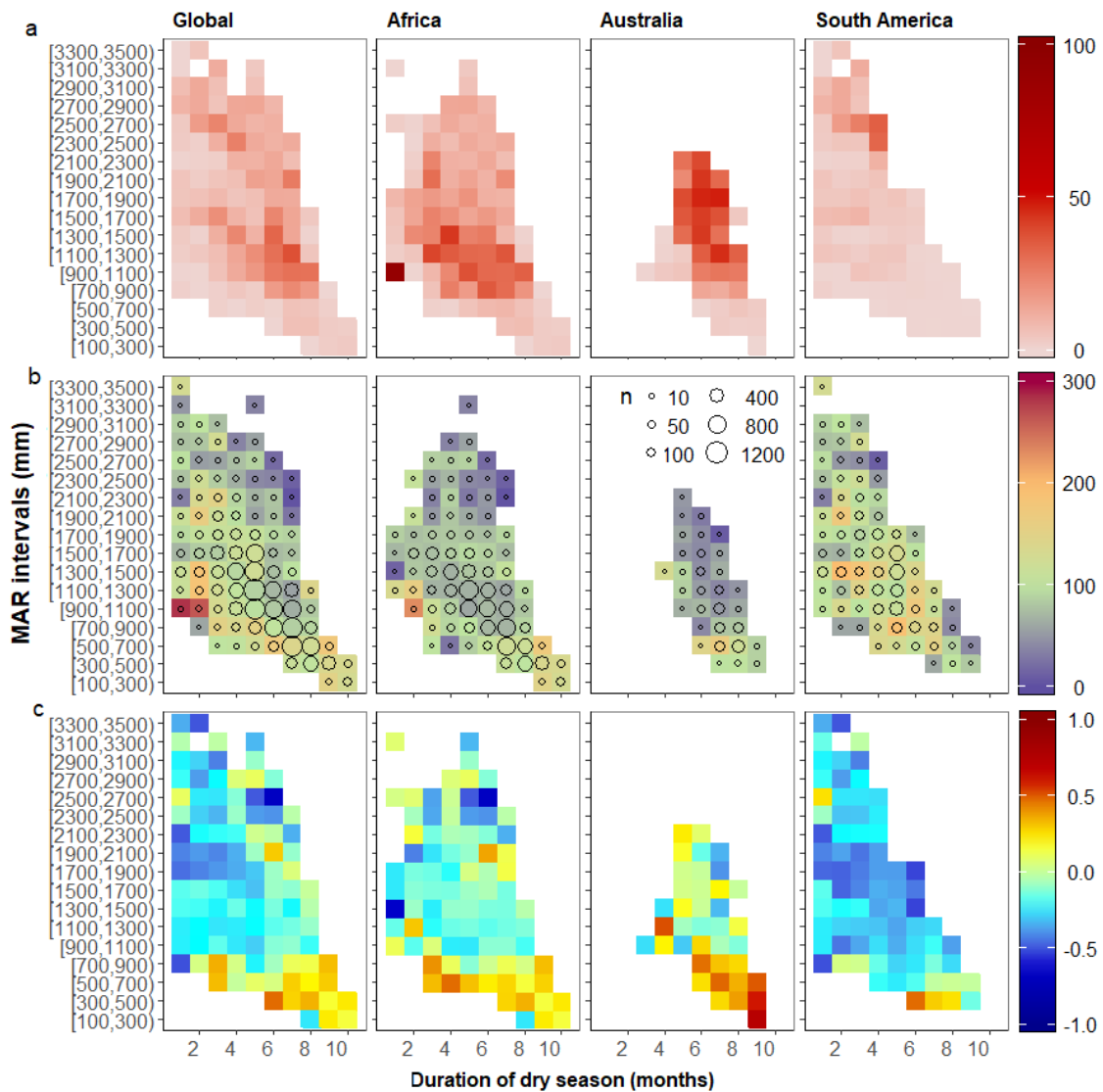
Fig. 3. Burned area response to dry season duration. (a) Median burned area (% yr^{-1}) per bin of Mean Annual Rainfall (MAR intervals) and dry season duration (b) Coefficient of variation of burned area per bin of Mean Annual Rainfall and dry season duration, circle size represent the upper limit of the number of grid cells by bin (n = number of grid cells). (c) Median correlation coefficient based on the per-pixel strongest absolute correlation within each bin of Mean Annual Rainfall and dry season duration. Cells with less than 3 pixels were excluded from panel b because the coefficients of variation calculate require at least 3 data.
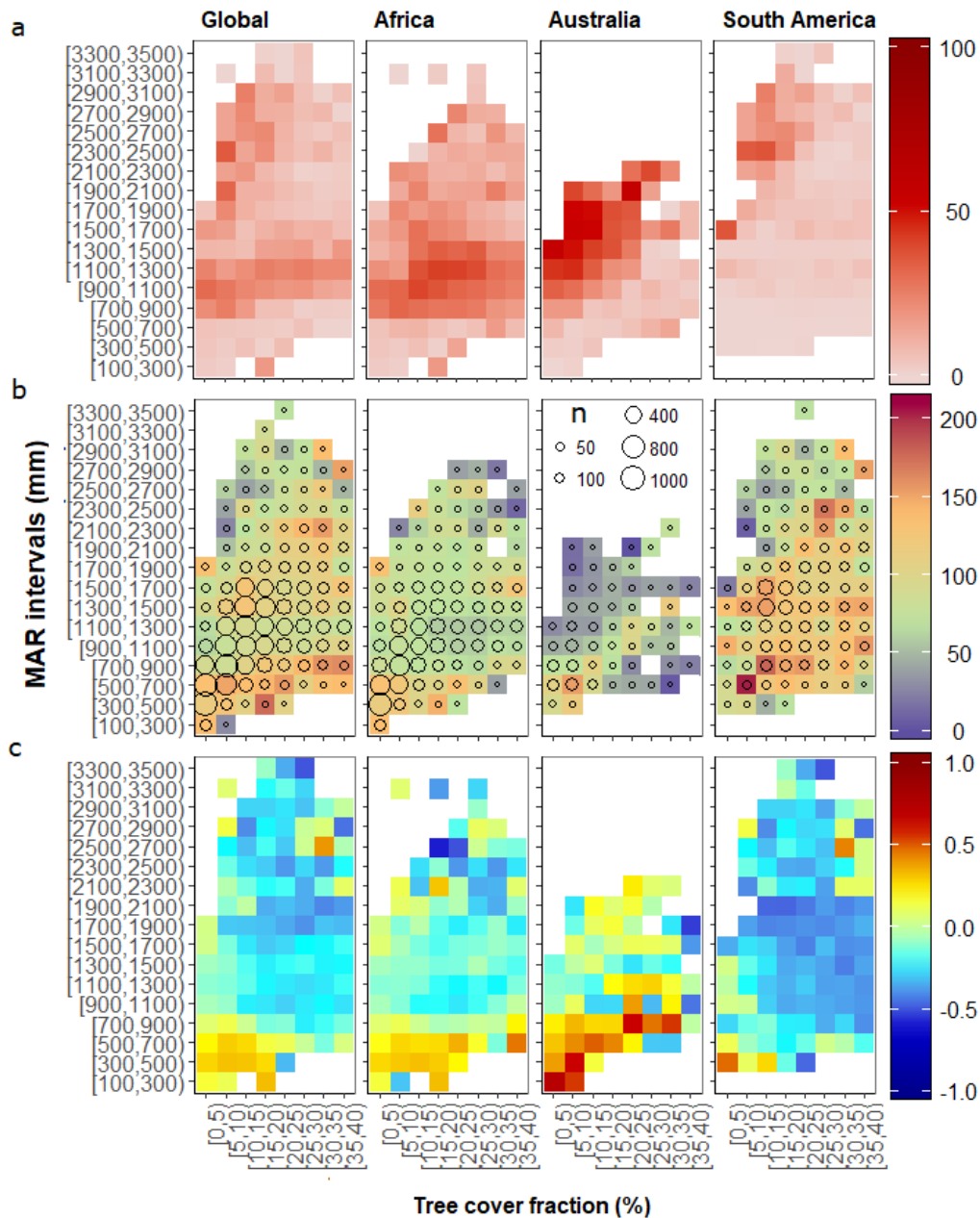
698

699

700

701
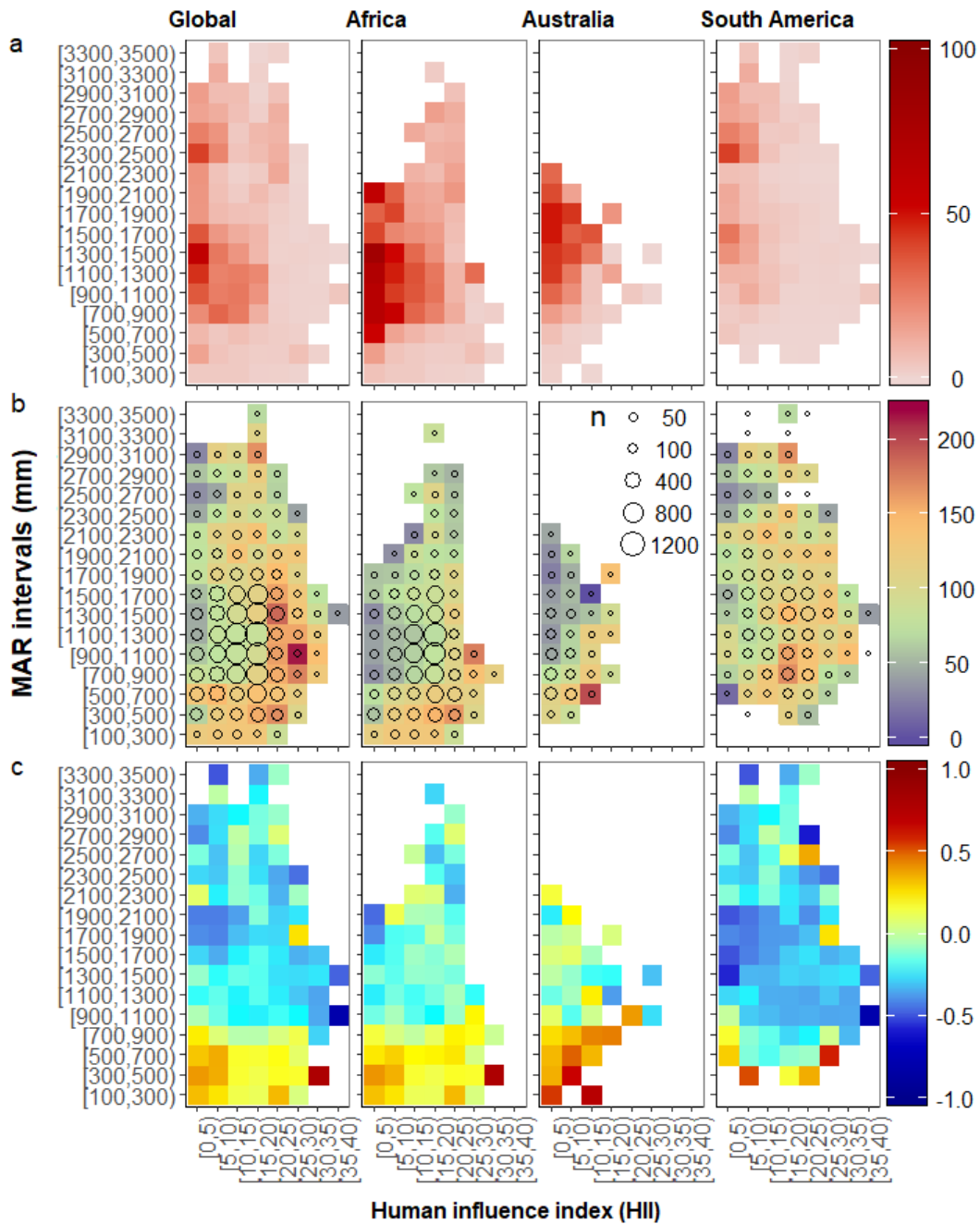
Fig. 4. Burned Area response to human land management. (a) Median burned area (% yr^{-1}) per bin of Mean Annual Rainfall (MAR intervals) and Human influence index. (b) Coefficient of variation of burned area per bin of Mean Annual Rainfall and Human influence index, circle size represent the upper limit of the number of grid cells by bin (n = number of grid cells). (c) Median correlation coefficient, based on the per-pixel strongest absolute correlation within each bin of Mean Annual Rainfall and Human influence index. Cells with less than 3 pixels were excluded from panel b because the coefficients of variation calculate require at least 3 data.

710

711

712

Fig. 5. Burned Area response to tree cover fraction. (a) Median burned area (% yr⁻¹) per bin of Mean Annual Rainfall (MAR intervals) and tree cover fraction (%). (b) Coefficient of variation of burned area per bin of Mean Annual Rainfall and tree cover fraction, circle size represent the upper limit of the number of grid cells by bin (*n* = number of grid cells). (c) Median correlation coefficient, based on the per-pixel strongest absolute correlation within each bin of Mean Annual Rainfall and tree cover fraction. Cells with less than 3 pixels were excluded from panel b because the coefficients of variation calculate require at least 3 data.